SUPPLEMENTARY INFORMATION FOR

Structural insight into the oxidation-sensing mechanism of the antibiotic resistance regulator MexR

Hao Chen[1+], Chengqi Yi[2], Jin Zhang[1], Wenru Zhang[3], Zhiyun Ge[1], Cai-Guang Yang[3++] & Chuan He[2+++]

[1]Coordination Chemistry Institute and the State Key Laboratory of Coordination Chemistry, School of Chemistry and Chemical Engineering, Nanjing University, Nanjing 210093, China, [2]Department of Chemistry and Institute for Biophysical Dynamics, The University of Chicago, 929 East 57th Street, Chicago, Illinois 60637, USA, [3]Shanghai Institute of Materia Medica, Chinese Academy of Sciences, 555 Zuchongzhi Road, Shanghai 201203, China

[+]Corresponding author. Tel: + 86 25 83621330; Fax: + 86 25 83621330; E-mail: chenhao@nju.edu.cn

[++]Corresponding author. Tel: + 86 21 50806029; Fax: + 86 21 50807088; E-mail: yangcg@mail.shcnc.ac.cn

[+++]Corresponding author. Tel: + 1 773 7025061; Fax: + 1 773 7020805; E-mail: chuanhe@uchicago.edu

Cloning, expression and purification of oxidized MexR

To improve diffraction quality, the C-terminus 5 amino acids truncated MexR (residues 1-142) was sub-cloned into Novagen pET30 between *Nde*I and *Xho*I sites. The expression and purification of the truncated MexR followed the previously published procedure (Chen *et al*, 2008). The purified MexR protein was incubated with stoichiometry mole ratio of 2,2′-dithiodipyridine at a concentration of 10 μM for 30 minutes at room temperature. After oxidation, the sample was purified by cation exchange chromatography(GE Healthcare, Mono S column, 1 mL, HR5/50 GL), and the fractions were identified by 14% non-reduced SDS-PAGE and combined for crystallization screening (Fig S1B online).

Structure determination

All diffraction data reduction was done using the HKL2000 suite of program (Otwinowski *et al*, 1997). Molecular replacement was conducted using the published apo-MexR structure (PDB 1LNW) as the template through the Phaser program from the CCP4 suite (Bailey, 1994). The structure model was manually built with COOT (Emsley *et al*, 2004). The program PyMOL was used in the production of the figures for publication (DeLano, 2002).

Modeling of oxidized MexR bound to dsDNA

Oxidized MexR was manually docked onto the OhrR operator DNA (Wilke *et al*, 2008). As shown in Fig S3, superimposition of apo-MexR dimer CD (PDB 1LNW) and DNA-bound OhrR from *Bacillus subtillus* (PDB 1Z9C) in PyMoL produced the model of DNA-bound dimer CD with a core rmsd of 3.4 $Å^2$. The relatively large

standard deviation mainly derives from the dimerization domain of each protomer, while their helix-turn-helix DNA-binding domains appear to recognize the DNA duplex, indicating that the models shown in Fig S3C and D are reasonable. Superimposition of oxidized MexR dimer on the DNA-bound CD dimer produced the oxidized MexR-DNA model. This is performed in PyMoL with one protomer from each dimer aligned to a core rmsd of 1.6 $Å^2$. As shown in Fig S3E and F, the spacing between the DNA binding domains is significantly reduced by ~7Å in the oxidized MexR dimer when compared to the reduced state of the CD dimer. Not enough space exists for the DNA helices to fit between the two protomers of the oxidized MexR.

Comparison of oxidized MexR with four reduced apo-MexR dimers

Conformational comparison of the four apo-MexR dimers (AB, CD, EF, and GH from PDB 1LNW) in reduced states and the oxidized MexR dimer is performed in PyMol, using all atoms from one protomer from each dimer (Fig S2). The core rmsd values are 2.4 $Å^2$, 1.6 $Å^2$, 1.8 $Å^2$, and 1.0 $Å^2$ for dimers AB, CD, EF, and GH, respectively. Dimerization helices α1′, α5′, and α6′ exhibit relatively small conformational changes, but the DNA-binding wing (β1 and β2) and helix-turn-helix motif (α2′ to α4′) undergo a large conformational change due to the formation of the disulfide bond. The movements are significant in these regions and exhibit fewer differences when the oxidized structure is compared with all four reduced structures. For example, the winged β1/β2 motif shifts around 6-8 Å, the N-termini of α1′ moves about 6-7 Å, and the N-termini of α5′ moves by 4-8 Å. It is hard to conclude which reduced dimer is closer to the conformation of the oxidized MexR.

The oxidation of Cys30 and Cys62

The purified MexRC30SC138S and MexRC62SC138S proteins (15 μM of protomer) were incubated with and without hydrogen peroxide for 60 minutes at 37 °C, respectively. Then, the excess amount of hydrogen peroxide was removed, and the samples were treated with 5,5'-dithio-bis(2-nitrobenzoic acid) (DTNB) to quantitatively determine free cysteines left. The oxidation ratio was calculated based on the UV-Vis recording at 280 nm and 412 nm (Fig S5K).

References

Bailey S (1994) The CCP4 suite: programs for protein crystallography. *Acta Crystallogr Sect D: Biol Crystallogr* **50:** 760-763

Chen H, Hu J, Chen PR, Lan L, Li Z, Hicks LM, Dinner A, He C (2008) The *Pseudomonas aeruginosa* multidrug efflux regulator MexR uses an oxidation-sensing mechanism. *Proc Natl Acad Sci USA* **105**: 13586-13591

DeLano WL (2002) The PyMOL molecular graphics system. DeLano Scientific LLC, Palo Alto, CA

Emsley P, Cowtan K (2004) Coot: model-building tools for molecular graphics. *Acta Crystallogr Sect D: Biol Crystallogr* **60:** 2126-2132

Otwinowski Z, Minor W (1997) Processing of X-ray diffraction data collected in oscillation mode. *Methods Enzymol* **276:** 307-326

Wilke MS, Heller M, Creagh AL, Haynes CA, Mclntosh LP, Poole K, Strynadka NCJ (2008) The crystal structure of MexR from *Pseudomonas aeruginosa* in complex with its antirepressor ArmR. *Proc Natl Acad Sci USA* **105**: 14832-14837

Rocchia W, Alexov E, Honig B (2001) Extending the applicability of the nonlinear Poisson-Boltzmann equation: Multiple dielectric constants and multivalent ions *J Phys Chem B* **105**: 6507-6514

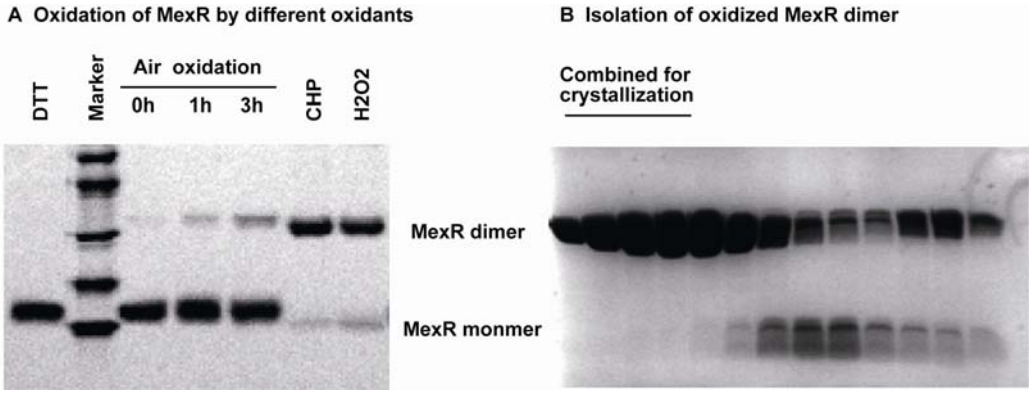

Fig. S1. Preparation and isolation of oxidized MexR. (*A*) Oxidation of MexR by different oxidants. The freshly purified wild-type MexR (5μM protomer) was exposed to air for up to 3 hours, or treated with 5 equivalents of CHP or H_2O_2 for 30 minutes, respectively. Then, the reaction was terminated by addition of excess iodoacetamide to quench the remaining free cysteines left. SDS-PAGE analysis was used to show the oxidation ratio. (*B*) Non-reducing SDS-PAGE analysis of the oxidized MexR after isolation. Oxidized MexR can be easily isolated from reduced MexR by ion exchange chromatography (GE Healthcare, 1 mL Mono S, HR 5/50 GL). The first four fractions were combined and concentrated to 10 mg/mL for crystallization experiments.

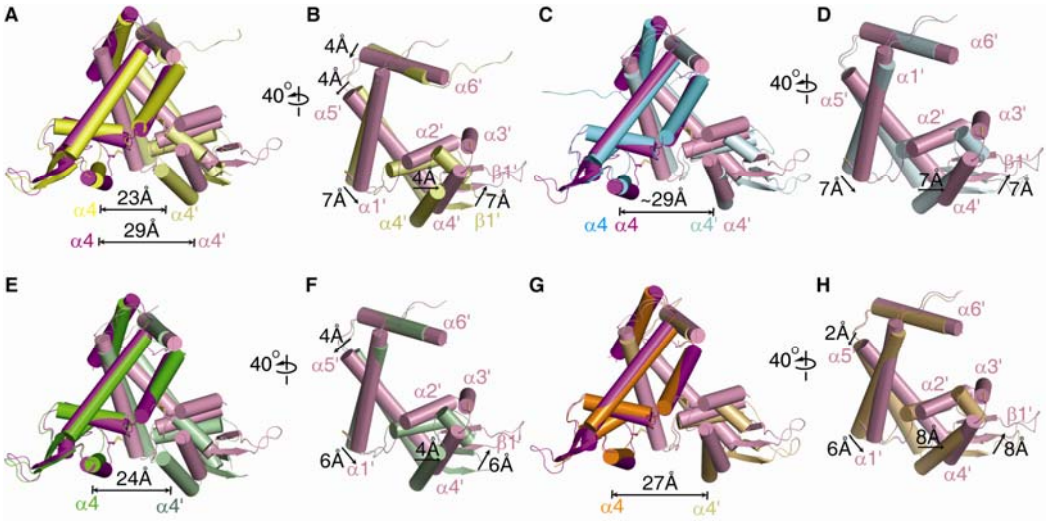

Fig. S2. Conformation comparison of the four apo-MexR dimers (AB, CD, EF, GH) in reduced state and the oxidized MexR dimer. All superimpositions were performed in PyMOL using all atoms from one protomer from each dimer. The oxidized dimer was colored in magenta and pink, AB in yellow and pale yellow, CD in cyan and pale cyan, EF in green and pale green, and GH in orange and light orange, respectively. The spacing between the DNA major-groove binding helices α4 and α4′ was shown. The motion of the DNA-binding wing (β1′ and β2′) and dimerization helices α1′, α5′, and α6′ for the oxidized MexR are indicated by arrows, and the shift distances were measured based on C_α-C_α distance for residues Arg85′ (*C*-termini of β1′), Arg32′ (*C*-termini of α1′), Asp99′ (*N*-termini of α5′), Phe121′ (*C*-termini of α5′), and Pro125′ (*N*-termini of α6′), respectively. (*A*) Superimposition AB dimer on the oxidized MexR with 2.4 $Å^2$ core rmsd. The spacing between the DNA major-groove binding helices α4 and α4′ was measured to be 23 Å in dimer AB, and 29 Å in the oxidized state, respectively. (*B*) Side view of the unaligned protomer as in *A*, rotated 40° to the right, highlighting the conformational differences in the helix-turn-helix

DNA-binding domains before and after oxidation. (*C*) Superimposition of the CD dimer on the oxidized MexR with 1.6 $Å^2$ core rmsd. The spacing between the DNA major groove binding helices α4 and α4′ was measured to be 29 Å for both the reduced and oxidized states. (*D*) Side view of the unaligned protomer as in *C*, rotated 40° to the right. (*E*) Superimposition of the EF dimer on the oxidized MexR with 1.8 $Å^2$ core rmsd. The spacing between the helices α4 and α4′ was measured to be 24 Å in the reduced dimer EF. (*F*) Side view of the unaligned protomer as in *E*, rotated 40° to the right. (*G*) Superimposition of the GH dimer on the oxidized MexR with 1.0 $Å^2$ core rmsd. The spacing between the helices α4 and α4′ is around 27 Å in the reduced dimer GH. (*H*) Side view of the unaligned protomer as in *G*, rotated 40° to the right.

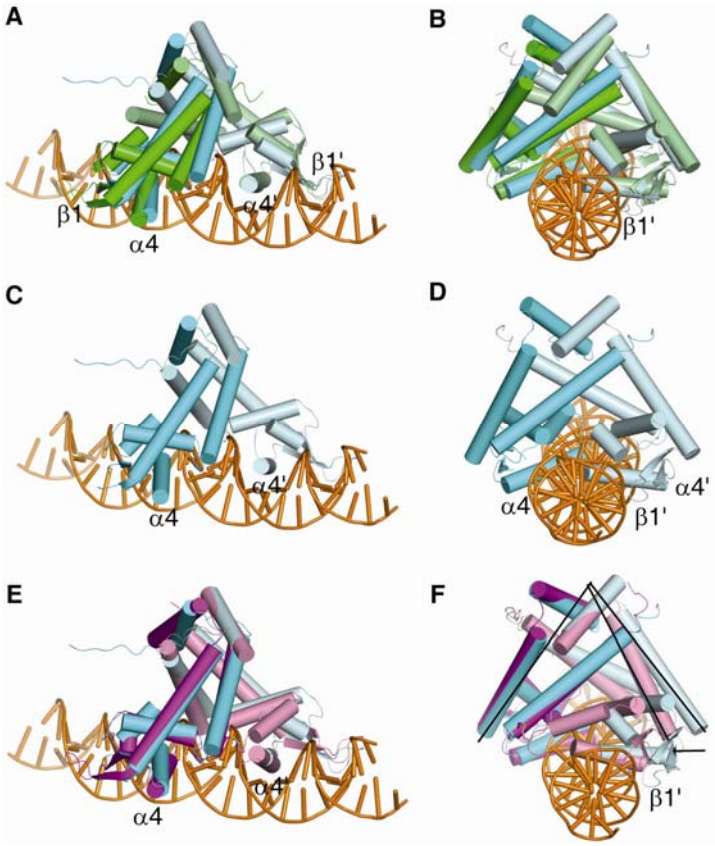

Fig S3. Docking of the oxidized MexR onto dsDNA. Superimpositions were performed in PyMol. The dsDNA is adopted from the complex of OhrR/DNA (PDB 1Z9C), and colored in orange. (*A*) Superimposition of the reduced MexR dimer CD (PDB 1LNW) and DNA-bound OhrR from *Bacillus subtillus* with a core rmsd of 4.9 $Å^2$. DNA-bound OhrR is colored in green and pale green. The position of the DNA major-groove binding helices α4 and α4′, and the minor-groove binding motives β1 and β1′ for both proteins are shown. (*B*) Side view of the aligned complex indicating a potential DNA-binding conformation of reduced MexR similar to OhrR. The minor-groove binding motif β1′ is shown. (*C*) Model of MexR CD dimer binding to DNA generated from *A* by removing the OhrR protein. (*D*) Side view of the model of CD dimer bound to DNA as in *C*. The DNA major-groove binding helices α4 and α4′,

and the minor-groove binding motif β1′ are labeled. (*E*) Alignment of the oxidized MexR and the model of the DNA-bound CD dimer in *C* (align one protomer on the left) with a core rmsd value of 1.6 $Å^2$. The DNA major-groove binding helices α4 and α4′ are labeled. (*F*) Side view of the superimposed complex as in *E*. The relative motion of the unaligned protomer in the oxidized MexR compared to that in the reduced dimer CD is indicated by the arrow. The minor-groove binding motif β1′ is indicated.

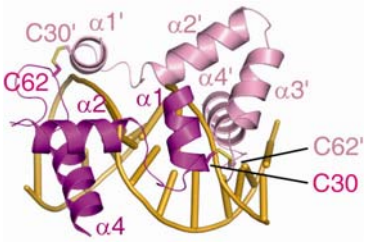

Fig. S4. Close up view of the model of the oxidized MexR bound to dsDNA as in Fig 2C and D. The disulfide bond between Cys30(′) and Cys62(′) is shown, which causes a clash mainly with the DNA backbone. The DNA major-groove-binding helices α4 and α4′ are still well positioned; however, α2 and α2′ also clash with DNA due to the introduction of disulfide bonds.

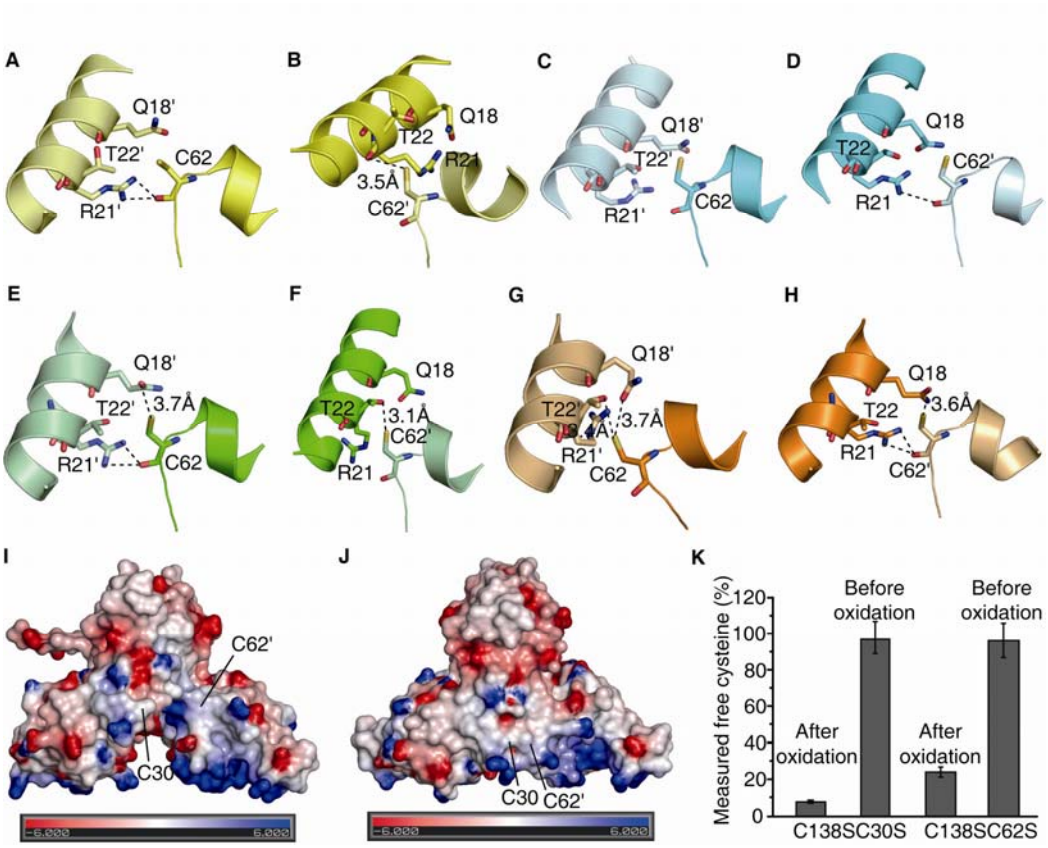

Fig. S5. Residues surrounding Cys30 and Cys62(′) and their relative oxidation. Hydrogen bonds are indicated with black dashed lines. The key residues, Gln18(′), Arg21(′), Thr22(′) and Cys62(′) are shown as sticks, and atoms are colored blue (nitrogen), red (oxygen), and yellow (sulfur). The same color coding was used as in Fig S2. Hydrogen bonding interactions in dimer AB (*A* and *B*), dimer CD (*C* and *D*), dimer EF (*E* and *F*), and dimer GH (*G* and *H*) were shown, respectively. All of these observed hydrogen-bonding interactions in the reduced MexR, including the carbonyl backbone of Arg21 to Cys62′ side chain (*B*), Gln18 side chain to Cys62′ side chain (*E*, *G*, and *H*), Thr22 side chain to Cys62′ side chain (*F* and *G*), come from residues from the other monomer, and contribute to lowering the *pKa* of Cys62(′). These interactions, together with the presence of two Arg residues nearby, may make

Cys62(′) more susceptible towards oxidation. Upon Cys62(′) oxidation to form the putative sulfenic acid, the disappearance of these interactions may contribute to the conformational change of MexR leading to the formation of disulfide bonds with Cys30. No direct hydrogen binding to Cys62 (′) in the reduced CD dimer is observed within 3.7 Å. (*I*) Electrostatic surface presentation of the reduced dimer CD. This was generated in DelPhi (Rocchia *et al*, 2001), showing basic residues surrounding Cys62′ and Cys30 in the reduced state, which might contribute to lowering the *pKa* of the thiol groups. The locations of these cysteines are indicated. (*J*) Electrostatic surface presentation around the disulfide bond region after MexR oxidation. (*K*) Oxidation activity test of Cys30 and Cys62 using DTNB assay. The quantification of the free cysteine was measured with UV-Vis spectroscopy, and presented as the height of dark gray bar. The standard deviation was calculated based on the average of three independent runs.

Table S1 Data collection and refinement statistics

	Oxidized MexR
Data collection	
Space group	P 21 21 21
Cell dimensions	
a, *b*, *c* (Å)	39.5, 72.2, 98.2
α, β, γ (°)	90, 90, 90
Resolution (Å)	50.0-2.1 (2.18-2.10) *
R_{sym}	0.055 (0.379)
$I/\sigma I$	26.4 (6.0)
Completeness (%)	99.7 (100)
Redundancy	7.1 (7.3)
Refinement	
Resolution (Å)	30.0-2.1 (2.15-2.10)
No. reflections	16091 (1132)
R_{work}/R_{free}	21.6/26.0 (23.4/32.9)
No. atoms	
Protein	2296
Water	100
B-factors	
Mean B value	38.1
R.m.s deviations	
Bond lengths (Å)	0.011
Bond angles (º)	1.369
Ramachandran Plot[#]	
Most favoured (%)	97.14
Allowed (%)	2.50
Disallowed (%)	0.36

*Highest resolution shell is shown in parenthesis.

[#]Values calculated in COOT.